

# COUPLED FIELD-STRUCTURAL ANALYSIS OF HTGR FUEL BRICK USING ABAQUS

Subhasish Mohanty,<sup>1</sup> Rajeev Jain,<sup>1</sup> Saurin Majumdar,<sup>1</sup> Timothy J. Tautges,<sup>1</sup> and Makuteswara Srinivasan <sup>2</sup>

<sup>1</sup>*Argonne National Laboratory, Argonne, Illinois*  
<sup>2</sup>*U.S. Nuclear Regulatory Commission, Washington, D.C.*

June 2012

The submitted manuscript has been created by UChicago Argonne, LLC, Operator of Argonne National Laboratory ("Argonne"). Argonne, a U.S. Department of Energy Office of Science laboratory, is operated under Contract No. DE-AC02-06CH11357. The U.S. Government retains for itself, and others acting on its behalf, a paid-up nonexclusive, irrevocable worldwide license in said article to reproduce, prepare derivative works, distribute copies to the public, and perform publicly and display publicly, by or on behalf of the Government.

To be presented in 2012 ICAPP Conference, Chicago, IL, June 24–28, 2012.

Portions of this work were supported by the U.S. Nuclear Regulatory Commission (US. NRC) under contract NRC Job Code V6218. This work also was supported in part by the U.S. Department of Energy, under Contract DE-AC02-06CH11357.

# COUPLED FIELD-STRUCTURAL ANALYSIS OF HGTR FUEL BRICK USING ABAQUS

Subhasish Mohanty,<sup>1</sup> Rajeev Jain,<sup>1</sup> Saurin Majumdar,<sup>1</sup> Timothy J. Tautges,<sup>1</sup> and Makuteswara Srinivasan<sup>2</sup>

<sup>1</sup>Argonne National Laboratory, Argonne, Illinois  
<sup>2</sup>U.S. Nuclear Regulatory Commission, Washington, D.C.  
Corresponding author email: smohanty@anl.gov

**Abstract** – High-temperature, gas-cooled reactors (HTGRs) are usually helium-gas cooled, with a graphite core that can operate at reactor outlet temperatures much higher than can conventional light water reactors. In HTGRs, graphite components moderate and reflect neutrons. During reactor operation, high temperature and high irradiation cause damage to the graphite crystal and grains and create other defects. This cumulative structural damage during the reactor lifetime leads to changes in graphite properties, which can alter the ability to support the designed loads. The aim of the present research is to develop a finite-element code using commercially available ABAQUS software for the structural integrity analysis of graphite core components under extreme temperature and irradiation conditions. In addition, the Reactor Geometry Generator toolkit, developed at Argonne National Laboratory, is used to generate finite-element mesh for complex geometries such as fuel bricks with multiple pin holes and coolant flow channels. This paper presents the proposed concept and discusses results of stress analysis simulations of a fuel block with H-451 grade material properties.

## I. INTRODUCTION

In a high-temperature, gas-cooled reactor (HTGR), numerous graphite blocks, or bricks, are used for reflecting neutron and containing fuel. Irradiation-induced dimension changes and creep play major roles in influencing the structural integrity of these bricks during sustained operation under extremely high temperature and neutron fluence.<sup>1-3</sup> Hence, for safe operation of HTGRs it is necessary to predict the time-dependent structural integrity of these components.

Structural integrity analysis is highly complex, involving interactive multiphysics conditions such as mechanical load, neutron dose, and heat transfer. In addition, the dependence of the nonlinear material properties on neutron dose and temperature further complicates the analysis.

The aim of the present research is to develop a coupled thermal-irradiation structural analysis code<sup>4-5</sup> using the commercially available ABAQUS software. Currently, ABAQUS cannot directly perform structural integrity analysis of graphite components under irradiation dose. A coupled field structural analysis code therefore is being developed at Argonne National Laboratory augmenting

ABAQUS with multiple user subroutines specifically developed for HTGR stress analysis<sup>6</sup>. In addition, in order to avoid using ABAQUS's graphical user interface (GUI) for mesh generation of complex geometry such as HTGR fuel bricks with fuel pin holes, we are using geometry mesh generated by the Reactor Geometry Generator (RGG) toolkit developed at Argonne.<sup>7</sup>

Discussed here is the current status of the coupled structural analysis code for conducting coupled field stress analysis of HTGR graphite components. Also presented are preliminary stress analysis results from a typical fuel brick in the General Atomics Gas turbine-modular helium reactor (GT-MHR)<sup>6</sup> HTGR configuration.

## II. FINITE ELEMENT MODEL DEVELOPMENT

A finite-element (FE) analysis procedure has been developed to perform the time-integrated stress analysis of the irradiated graphite component. The details of the FE model are discussed below.

### II.A. Irradiation Graphite Constitutive Relation

Nuclear reactor graphite components subjected to irradiation can be modeled by using the Maxwell-Kelvin linear visco-elastic creep model.<sup>1</sup> Under HTGR reactor conditions, the total strain in graphite can be from different sources, such as elastic strain ( $\epsilon^e$ ), irradiation primary creep strain ( $\epsilon^{ipc}$ ), irradiation secondary creep strain ( $\epsilon^{isc}$ ), irradiation dimensional change strain ( $\epsilon^{idim}$ ), and thermal strain ( $\epsilon^\theta$ ). Since current HTGRs are designed to operate at temperatures below 2000 °C, one can assume that the contributions from primary thermal creep strain ( $\epsilon^{\theta pc}$ ) and secondary thermal creep strains ( $\epsilon^{\theta sc}$ ) are negligible in graphite components. Figure 1 shows a schematic representation of the individual strain elements of graphite component under irradiation condition.

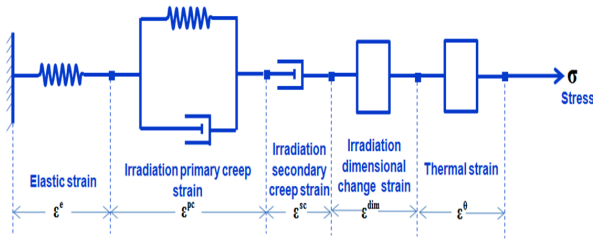


Fig. 1. Schematic representation of various strains.

If we assume for simplicity that primary creep strain is negligible compared with secondary creep strain at moderate to high doses<sup>8</sup> and that the temperature remains constant ( $\epsilon^\theta \approx 0$ ), then the total strain ( $\epsilon^t$ ) in an HTGR core graphite component can be represented as

$$\epsilon^t = \epsilon^e + \epsilon^{isc} + \epsilon^{idim} \quad (1)$$

The corresponding three-dimensional stress-strain relations can be given as

$$\sigma = C^{ie} \epsilon^e = C^{ie} (\epsilon^t - \epsilon^{isc} - \epsilon^{idim}), \quad (2)$$

where  $C^{ie}$  is the time-dependent, irradiated elastic matrix that depends on the temperature and fluence-dependent irradiation material properties.

### II.B. Finite-Element Model

A finite-element code for HTGR stress analysis is being developed at the Nuclear Engineering Division of Argonne National Laboratory. For this purpose, the commercially available ABAQUS software is being augmented with user material (UMAT) subroutines specifically developed in-

house to meet the present stress analysis requirements. UMAT calculates the time- and space-dependent irradiation material properties based on fluence and temperature at each integration point of the individual elements. Based on these material properties, the material stiffness matrix  $C^{ie}$  and the corresponding stress and strains are updated. The ABAQUS finite-element implementation is schematically presented in Fig. 2.

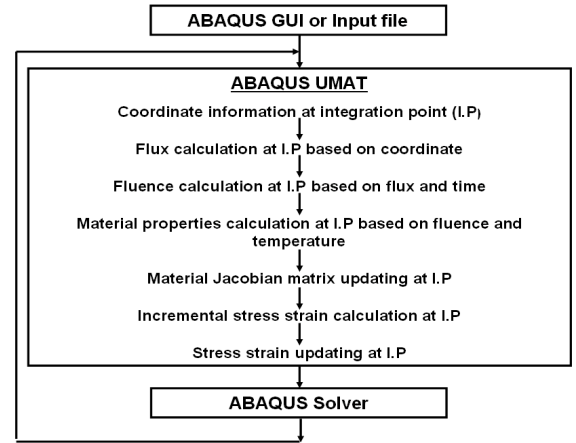


Fig. 2. Schematic of ABAQUS UMAT implementation.

### III. NUMERICAL RESULTS

The ABAQUS-based FE code was used to perform stress analysis of a typical fuel brick using realistic material properties and realistic fluence profiles. For stress analysis, the GT-MHR core with hexagonal fuel brick geometry<sup>5</sup> was considered. The location of the fuel brick for the present FE simulation can be seen from Fig. 3.

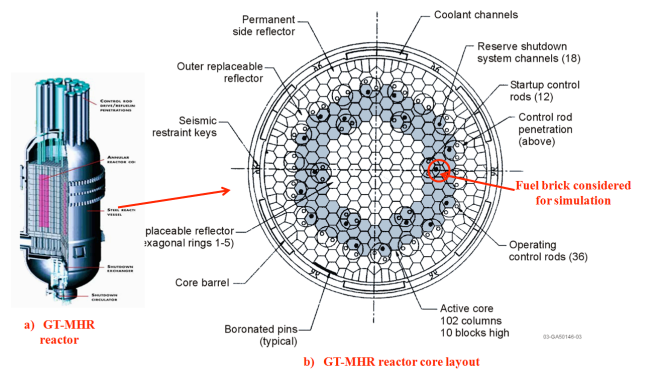


Fig. 3. Location of the fuel brick in GT-MHR reactor layout for the present simulation, with the fuel brick center located 195.67 cm from the center of reactor core.

The details of the finite-element mesh, fluence profile, material properties, and stress analysis results are discussed in the following subsections.

### III.A. Finite-Element Mesh

Using the ABAQUS GUI for mesh generation of graphite blocks with fuel pin holes is complex. In order to avoid this complexity, the fuel brick geometry and mesh were generated by using the Argonne-developed Reactor Geometry Generator toolkit.<sup>7</sup> RGG is a part of MeshKit,<sup>9</sup> an open-source mesh-generating software kit being developed and maintained at Argonne. The RGG toolkit consists of two major components: AssyGen and CoreGen. AssyGen is used to develop assembly geometry and journal files to generate mesh on the corresponding geometry; CoreGen moves several such assembly geometries or mesh files to create the core model. These tools can be used to model core geometry for several different types of reactors, such as pressurized water reactors, boiling water reactors and very high temperature reactors.

The RGG uses a three-stage process to create the core models, Stage 1 is AssyGen, Stage 2 is meshing, and Stage 3 is CoreGen. In the second stage, the meshing script and geometry output from AssyGen are used to generate a mesh for that assembly type. This process of constructing assembly meshes, while somewhat automated, can be sensitive to mesh size input. The problem is manifested particularly in the generation of unstructured quadrilateral meshes for the top surface in an assembly, which is cut by large numbers of cylindrical rods. To keep the overall mesh sizes reasonable, analysts typically choose one or two quadrilateral elements between fuel rods; however, meshing with such relatively coarse sizes (compared with the geometric features in the region) will often be futile. This is one of the reasons for splitting the core mesh generation process into several steps, thereby allowing user intervention midway through the process.

For the fuel brick model, the AssyGen tool was used. The fuel block pitch is assumed to be 36 mm, similar to that of the GT-MHR fuel block pitch length.<sup>5</sup> In order to expedite the present simulation, however, the height of the brick was reduced from the original 793 to 7.93 mm. Simulation of a full -length brick is one of our future tasks. Various mesh sizes were tried by changing the "template.jou" file generated by AssyGen. The overall size of the mesh is sensitive to the number of divisions in the Z-direction. The number of meshes in the Z-direction was restricted to 4 for this problem. Generation of the geometry and meshing script took 40 seconds on a Linux desktop. Figure 4 shows the FE mesh generated by the RGG toolkit.

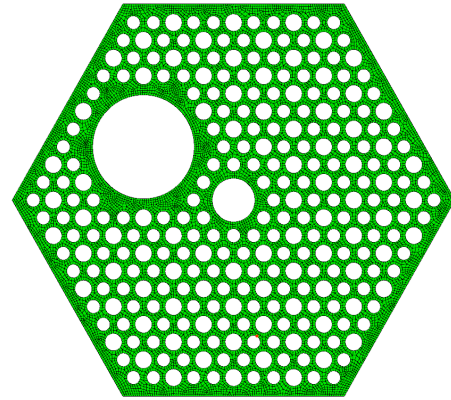


Fig. 4. FE mesh of fuel brick, generated using the RGG/AssyGen tool.

### III.B. Fluence Profile Calculation

The finite-element code requires time-dependent fluence information at each integration point of the individual finite element. If one assumes that the neutron flux  $\psi$  remains constant, then the fluence at a particular location can be expressed as

$$\gamma = \psi t, \quad (3)$$

where  $\gamma$  is the fluence,  $t$  is the time in seconds, and  $\psi$  is the neutron flux at a particular integration point in  $\text{n/cm}^2$ . The flux at any location can be determined by an exponential function given by the following.

$$\psi = e^{(C_0 + C_1 r + C_2 r^2 + C_3 r^3 + C_4 r^4 + C_5 r^5)} \quad (4)$$

Here,  $r$  is the radial distance of the integration point from the center of the core. The parameters  $C_{i=0K5}$  can be estimated by fitting the flux profile estimated from thermo-hydraulics calculations. In the present analysis, the flux profile reported by Idaho National Laboratory<sup>10</sup> was used for estimating  $C_{i=0K5}$ . Figure 5 shows the original flux profile and the regenerated flux profile estimated by Eq. 4. Figures 6, 7, and 8 show the fluence distribution in a typical fuel brick, calculated by ABAQUS UMAT at the end of 1, 3, and 4.5 years of reactor operation, respectively. The fluence distributions are shown in dpa ( $1 \text{ dpa} = 0.78 \times 10^{21} \text{ n/cm}^2$ ) scale.

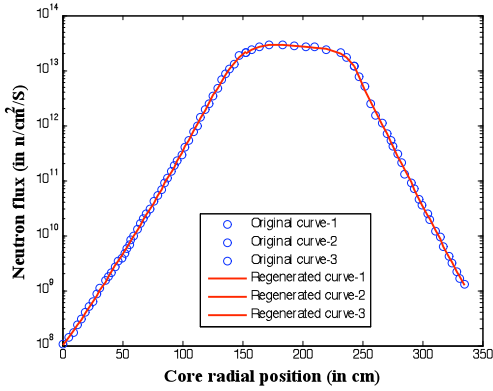


Fig. 5. Flux profile with respect to distance from the center of core.

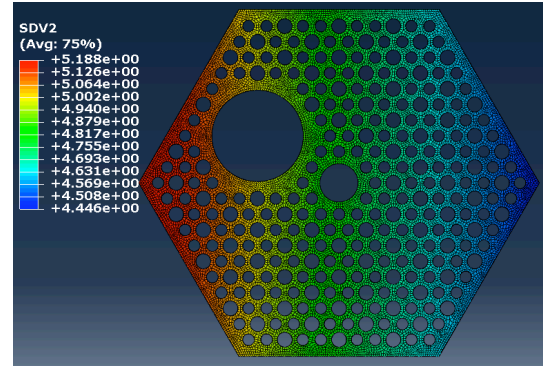


Fig. 8. Irradiation dose in dpa at the end of 4.5 years of reactor operation.

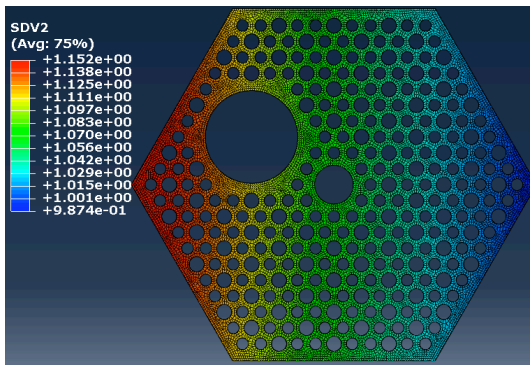


Fig. 6. Irradiation dose in dpa at the end of one year of reactor operation.

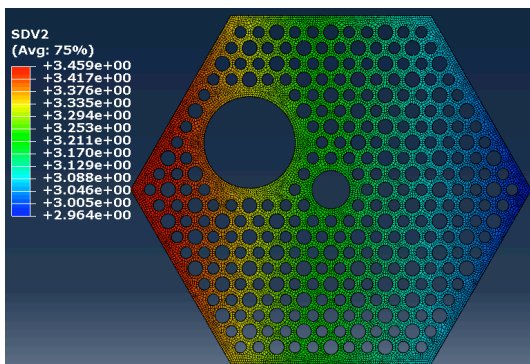


Fig. 7. Irradiation dose in dpa at the end of 3 years of reactor operation.

### III.C. Material Properties Model

Transversely isotropic H-451 graphite grade material properties were considered for the present simulation. The material properties data were generated at Oak Ridge National Laboratory and are publicly available through the *Graphite Design Handbook* published by General Atomics.<sup>3</sup> The FE simulation was performed assuming a constant temperature of 900 °C. Poisson’s ratio for all the elastic materials is assumed to be constant and equal to 0.2, and Poisson’s ratio in creep is assumed to be constant and equal to 0.5. Unlike Poisson’s ratio, Young’s modulus in irradiated specimens is assumed to be fluence dependent. Figure 9 shows Young’s modulus in axial and radial directions used in the present simulation. In addition, for the present work, Young’s modulus used for calculating the creep compliance matrix was assumed equal to Young’s modulus for irradiated materials. Figures 10a and 10b show the ABAQUS UMAT-calculated axial and radial Young’s modulus, respectively, at the end of 1 year of irradiation. Similarly Figures 11 and 12 show the Young’s modulus distribution at the end of 3 and 4.5 years, respectively.

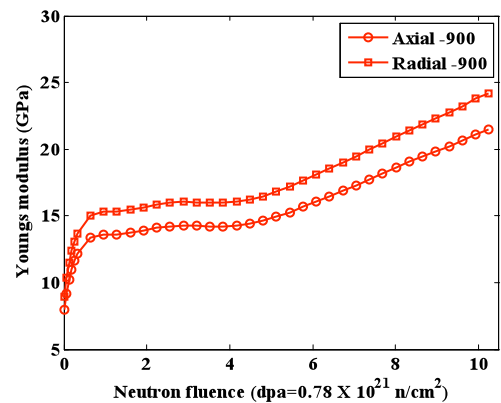


Fig. 9. Irradiated Young’s modulus with respect to fluence and orientation

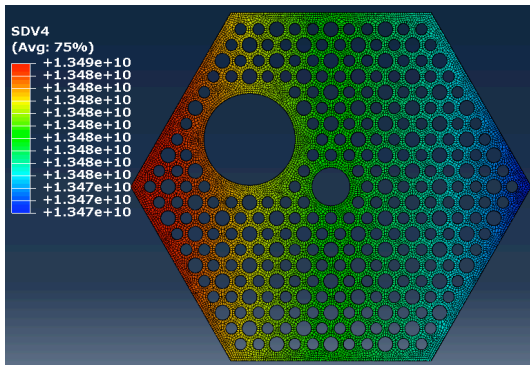


Fig. 10a. Axial Young's modulus (in  $N/m^2$ ) distribution at the end of 1 year of irradiation.

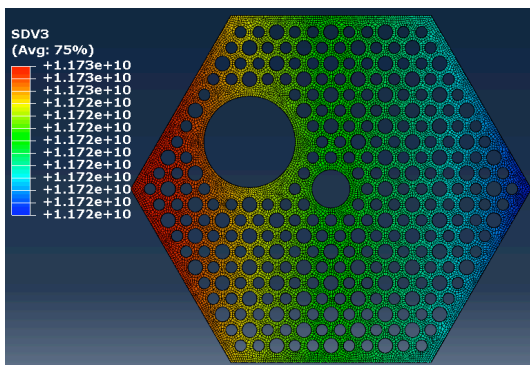


Fig. 10b. Radial Young's modulus (in  $N/m^2$ ) distribution at the end of 1 year of irradiation.

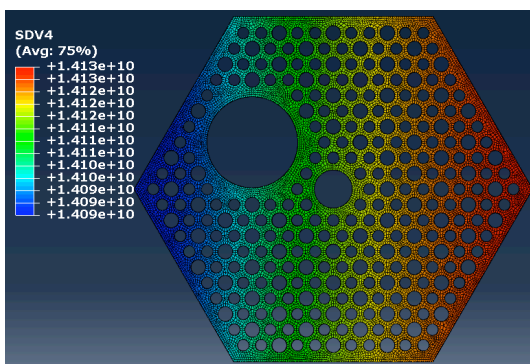


Fig. 11a. Axial Young's modulus (in  $N/m^2$ ) distribution at the end of 3 years of irradiation.

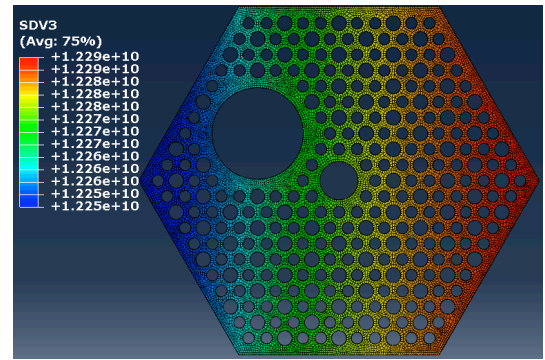


Fig. 11b. Radial Young's modulus (in  $N/m^2$ ) distribution at the end of 3 years of irradiation.

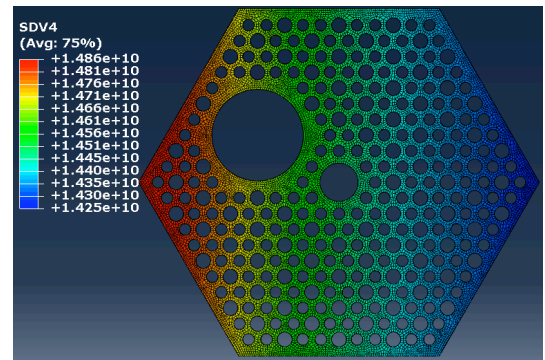


Fig. 12a. Axial Young's modulus (in  $N/m^2$ ) distribution at the end of 4.5 years of irradiation.

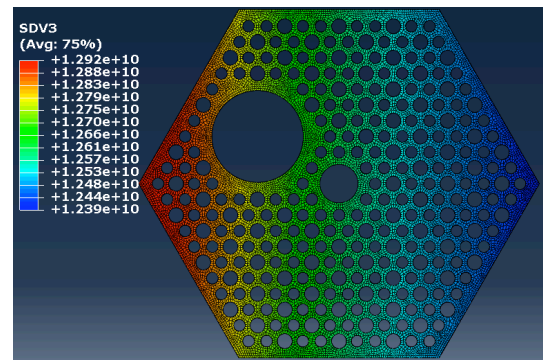


Fig. 12b. Radial Young's modulus (in  $N/m^2$ ) distribution at the end of 4.5 years of irradiation.

UMAT requires irradiation dimensional change strain data as input. The data used for the present simulation were based on the design curves given in the *Graphite Design Handbook*.<sup>3</sup> Figure 13 shows the irradiation dimensional change strain data for H-451 graphite at 900 °C. Based on this dimensional change strain vs. fluence plot, ABAQUS UMAT calculated the dimensional change strain at each integration point. Figures 14a and 14b show the axial and radial dimensional change strain distributions, respectively, in the fuel brick as calculated by ABAQUS. Similarly,

Figs. 15 and 16 show the dimensional change distribution at the end of 3 and 4.5 years, respectively.

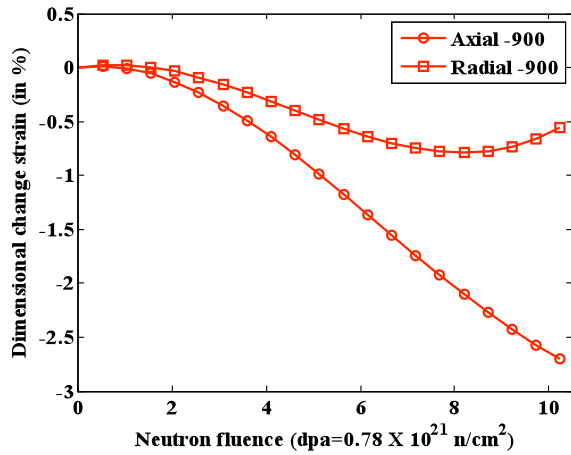


Fig. 13. Dimensional change strain design curves for H-451 grade graphite.

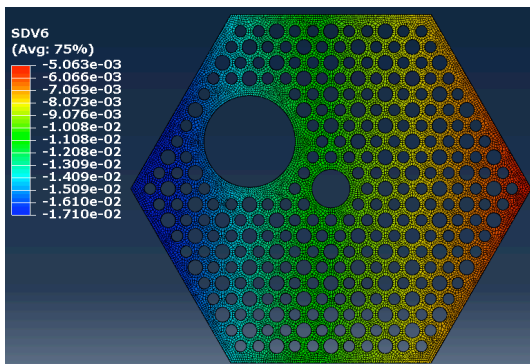


Fig. 14a. Axial dimensional change strain distribution at the end of 1 year of irradiation.

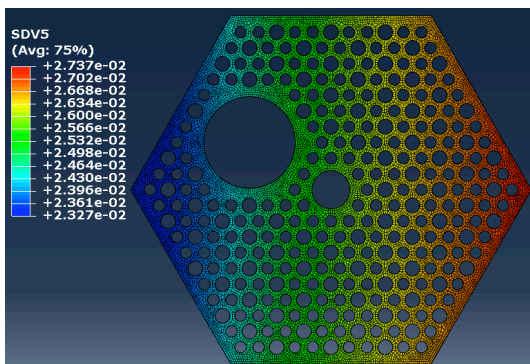


Fig. 14b. Radial dimensional change strain distribution at the end of 1 year of irradiation.

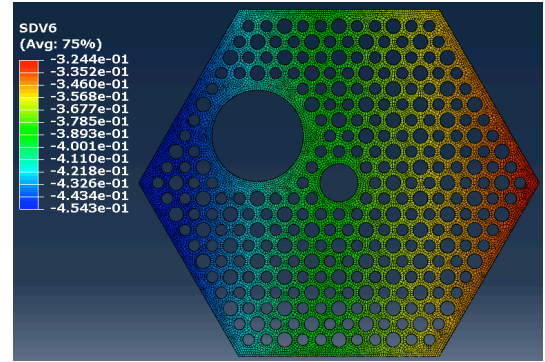


Fig. 15a. Axial dimensional change strain distribution at the end of 3 years of irradiation.

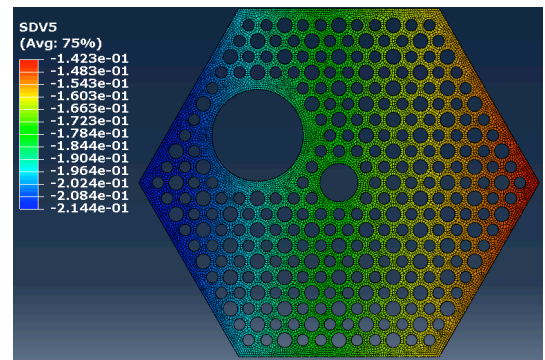


Fig. 15b. Radial dimensional change strain distribution at the end of 3 years of irradiation.

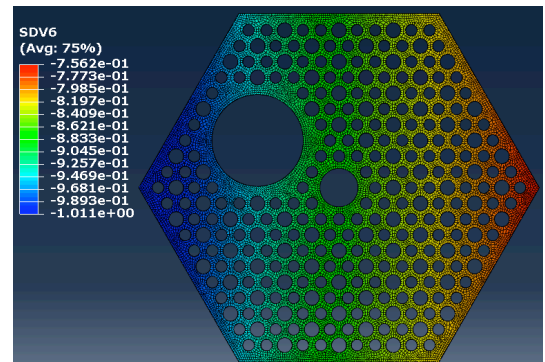


Fig. 16a. Axial dimensional change strain distribution at the end of 4.5 years of irradiation.

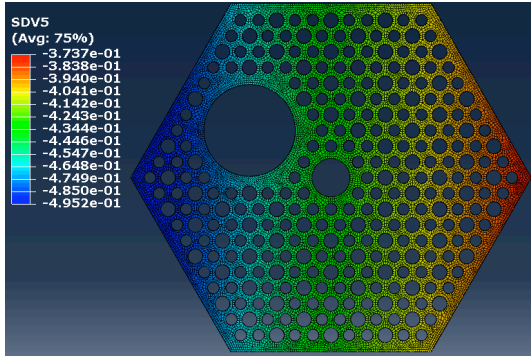


Fig. 16b. Radial dimensional change strain distribution at the end of 4.5 years of irradiation.

### III.D. Stress Results

Based on the material properties and fluence distribution discussed above, a time-integrated stress analysis was performed for the fuel brick. Figure 17 shows the time-history of maximum principal stress at two extreme ends of the fuel brick. In all the figures showing fuel block cross-section, the leftmost vertex is toward the center of the core (i.e., nearest point), and the rightmost vertex is away from the core center (i.e. farthest point). It can be seen from Fig. 17 that the stresses at the nearest point to the core are higher than those at the farthest point. The reason is that the nearest point experiences higher dimensional change strain compared with the farthest point, caused by the higher dose at the nearest point compared with that at the farthest point, as evident in Figs. 6-8. Figures 18 and 19 show the spatial distributions of maximum principal stress at the end of 3 and 4.5 years of irradiation exposure, respectively. From these figures it can be seen that the location of the maximum stress is around the control rod channel. Fig. 18 shows that the maximum principal stress is approximately 21.5 MPa at the end of 3 years and Fig. 19 shows that the maximum principal stress at the end of 4.5 years is approximately 29.3 MPa. Figure 20 shows the change in irradiated strength relative to unirradiated strength as a function of fluence and temperature. For a simulation temperature of 900 °C, the strength ratios at 3.5 and 5.2 fluence doses are approximately 1.45 and 1.55, respectively. For reference, the average unirradiated strengths of H-451 graphite are reported in the literature<sup>11</sup> as: mean tensile strength = 15 MPa, mean compressive strength = 55 MPa, and mean flexural strength = 27 MPa. Using the fluence data reported in Figs 7 and 8 and Fig. 20, the irradiated ultimate (tensile) strengths of the fuel brick at the end of 3 and 4.5 years are 21.8 MPa and 23.3 MPa, respectively. Comparing the predicted maximum principal stress with the irradiated strength, the approximated factor of safety at the end of 3 and 4.5 years can be found as 1.01 and 0.79, respectively. This type of simulation will help the designer to schedule the inspection/replacement intervals of the fuel and reflector bricks depending on the required

factor of safety. However, the safety factor calculated above may not be adequate. For more accurate prediction, more detail simulations and better irradiation material properties are needed. It is also recognized that such high stresses are highly localized and that probability of failure of the entire brick estimation involves calculations using probabilistic stress analysis integrating the stress of individual elements of the entire brick. Such calculations are beyond the scope of this current work.

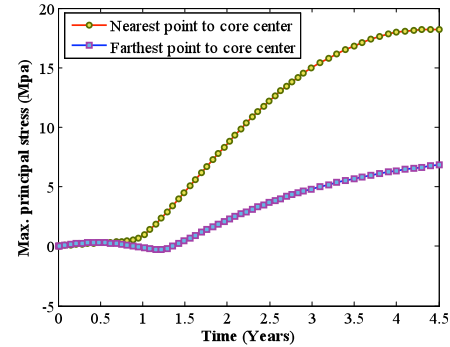


Fig. 17. Maximum principal stress with respect to time at two extreme (nearest and farthest element) element from the core center.

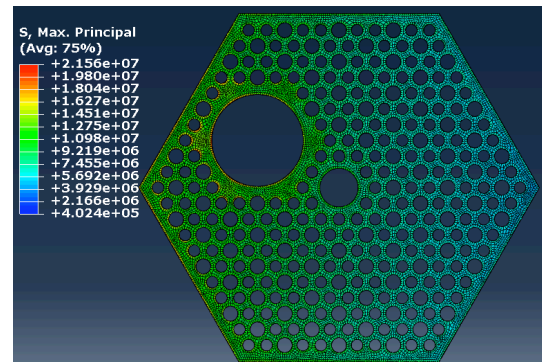


Fig. 18. Maximum principal stress (N/m<sup>2</sup>) at the end of 3 years of irradiation exposure.

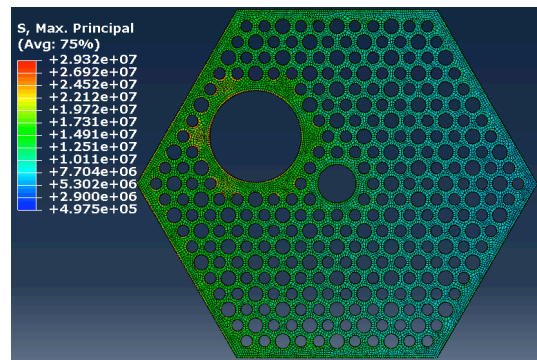


Fig. 19. Maximum principal stress (N/m<sup>2</sup>) at the end of 4.5 years of irradiation exposure.

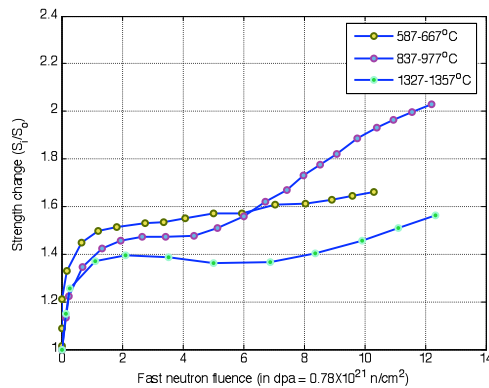


Fig. 20. Irradiation strength data for H-451 graphite.<sup>12</sup>

#### IV. CONCLUSIONS

An ABAQUS software-based, finite-element analysis procedure is presented for stress analysis of high-temperature, gas-cooled reactor core graphite components. The code currently can account for irradiation-induced dimensional change strain and creep and will include thermal strain effects in the future. The code has been demonstrated to be capable of carrying out stress analysis for a realistic HTGR component with realistic reactor conditions. For the numerical simulation, a typical fuel brick of GT-MHR reactor was considered. The stress analysis was demonstrated with transversely isotropic H-451 grade material properties and a GT-MHR core fluence profile. The simulations indicate that the maximum stresses in the fuel brick may be within the design margin for up to 3 years of operation. For a more accurate evaluation, a more detailed simulation considering detailed geometry, irradiated material properties, geometric and field boundary conditions are needed. Equally important, irradiated material properties data needs to be generated for the HTGR candidate materials. The developed procedure can be extended to perform stress and structural integrity analysis of other fuel bricks and reflector bricks and for the analysis of the complete or whole core with multiple bricks.

#### ACKNOWLEDGMENTS

Portions of the work were supported by the U.S. Nuclear Regulatory Commission (US. NRC) under contract NRC Job Code V6218 during FY2011. This work also was supported in part by the U.S. Department of Energy, under Contract DE-AC02-06CH11357.

#### DISCLAIMER

This paper was prepared as an account of work sponsored by an agency of the U.S. Government. Neither the U.S. Government nor any agency thereof, nor any of their employees, makes any warranty, expressed or implied, or assumes any legal liability or responsibility for any third party's use, or the results of such use, of any information, apparatus, product, or process disclosed in this report, or represents that its use by such third party would not infringe privately owned rights. The views expressed in this paper are not necessarily those of the U.S. Nuclear Regulatory Commission.

#### NOMENCLATURE

$\mathbf{C}^{ie}$	: Irradiation stiffness matrix
$\mathbf{g}$	: Neutron fluence (n/cm <sup>2</sup> )
$\boldsymbol{\varepsilon}^e$	: Elastic strain
$\boldsymbol{\varepsilon}^t$	: Total strain
$\boldsymbol{\varepsilon}^{ipc}$	: Irradiation primary creep strain
$\boldsymbol{\varepsilon}^{isc}$	: Irradiation secondary creep strain
$\boldsymbol{\varepsilon}^{idim}$	: Irradiation dimensional change strain
$\boldsymbol{\sigma}$	: Stress vector
$\psi$	: Neutron flux (n/cm <sup>2</sup> /S)

#### REFERENCES

1. R. J. Price, Irradiation-Induced Creep in Graphite: A Review. GA-A16402, General Atomics Company, CA (1981).
2. T. D. Burchell, Irradiation induced creep behavior of H-451 graphite, *Journal of Nuclear Materials*, 381, 1-2, 46-54 (2008).
3. *Graphite Design Handbook*, DOE-HTGR-88111, General Atomics Company, CA (1988).
4. D K L. Tsang, and B J., Marsden, "The development of a stress analysis code for nuclear graphite components in gas-cooled reactors", *Journal of Nuclear Materials*, 350, 3, (2006).
5. R. L. Bratton, *Modeling Mechanical Behavior of a Prismatic Replaceable Reflector Block*. INL/EXT-09-15868, Idaho National Laboratory, Idaho Falls, ID, (2009).
6. S. Mohanty and S. Majumdar, HTGR Graphite Core Component Stress Analysis Research Program – Task 1 Technical Letter Report, NRC, ML11276A009, 2011.

7. T. J. Tautges and R. Jain, Creating geometry and mesh models for nuclear reactor core geometries using a lattice hierarchy-based approach, *Journal of Engineering with Computers* (2011).
8. H. Li, A. S. L. Fox., and B. J. Marsden, An analytical study on the irradiation-induced stresses in nuclear graphite moderator bricks, *Journal of Nuclear Materials*. 372, 164–170 (2007).
9. Argonne MeshKit website (2012) <http://trac.mcs.anl.gov/projects/fathom/browser/MeshKit>
10. J. W. Sterbentz, Calculated neutron and gamma-ray spectra across the prismatic very high temperature reactor core, pp. 596–606 in *Reactor Dosimetry State of the Art 2008*, edited by W. Voorbraak, P. D'hondt, and J. Wagemans, World Scientific (2008).
11. Y. S. Virgil'ev and I. P. Kalyagina, Reactor graphite, *Inorganic Materials Journal*, 39, 1, S46–S58 (2003).
12. R. J. Price and L. A. Beavan, *Final Report on Graphite Irradiation Test*, OG-1. GA-A13089, General Atomics Company, CA (1974).